Molecular Neurobiology (2018) 55:8001–8013
https://doi.org/10.1007/s12035-018-0965-4

ORIGINAL PAPER

Physiological Concentration of Prostaglandin E_2 Exerts Anti-inflammatory Effects by Inhibiting Microglial Production of Superoxide Through a Novel Pathway

Shih-Heng Chen[1] · Yueh-Feng Sung[1,2] · Esteban A. Oyarzabal[1] · Yu-Mei Tan[3] · Jeremy Leonard[4] · Mingri Guo[1,5] · Shuo Li[1,6] · Qingshan Wang[1] · Chun-Hsien Chu[1] · Shiou-Lan Chen[7] · Ru-Band Lu[8,9] · Jau-Shyong Hong[1]

Received: 24 August 2017 / Accepted: 16 February 2018 / Published online: 1 March 2018

Abstract

This study investigated the physiological regulation of brain immune homeostasis in rat primary neuron-glial cultures by sub-nanomolar concentrations of prostaglandin E2 (PGE_2). We demonstrated that 0.01 to 10 nM PGE_2 protected dopaminergic neurons against LPS-induced neurotoxicity through a reduction of microglial release of pro-inflammatory factors in a dose-dependent manner. Mechanistically, neuroprotective effects elicited by PGE_2 were mediated by the inhibition of microglial NOX2, a major superoxide-producing enzyme. This conclusion was supported by (1) the close relationship between inhibition of superoxide and PGE_2-induced neuroprotective effects; (2) the mediation of PGE_2-induced reduction of superoxide and neuroprotection via direct inhibition of the catalytic subunit of NOX2, $gp91^{phox}$, rather than through the inhibition of conventional prostaglandin E2 receptors; and (3) abolishment of the neuroprotective effect of PGE_2 in NOX2-deficient cultures. In summary, this study revealed a potential physiological role of PGE_2 in maintaining brain immune homeostasis and protecting neurons via an EP receptor-independent mechanism.

Keywords Prostaglandin E_2 · Microglia · NOX2 · Neuroprotection · Neuro-inflammation

Introduction

Prostaglandin E_2 (PGE_2) exhibits diverse hormone-like effects in animals, acting through a wide range of physiological targets and mechanisms, such as neurons, smooth muscles, secretary cells, and immune function [1–3]. Immune function of PGE_2 in modulating neuro-inflammation has been an active area of research, but the roles of PGE_2 as a pro-inflammatory or anti-inflammatory mediator are far from clear. Under normal conditions, a modest level of PGE_2 is produced in neurons, microglia, and astroglia; however, a large amount of PGE_2 is produced mainly by microglia during neuro-

Electronic supplementary material The online version of this article (https://doi.org/10.1007/s12035-018-0965-4) contains supplementary material, which is available to authorized users.

✉ Shih-Heng Chen
chens3@niehs.nih.gov

✉ Jau-Shyong Hong
hong3@niehs.nih.gov

[1] Neurobiology Laboratory, National Institute of Environmental Health Sciences, National Institutes of Health, NIEHS/NIH, 111 T.W. Alexander Dr., Research Triangle Park, NC 27709, USA

[2] Department of Neurology, Tri-Service General Hospital, National Defense Medical Center, Taipei, Taiwan

[3] U.S. Environmental Protection Agency, National Exposure Research Lab, Research Triangle Park, NC, USA

[4] Oak Ridge Institute for Science and Education, Oak Ridge, TN, USA

[5] Department of Laboratory Medicine, Tianjin Haihe Hospital/Haihe Clinical Institute of Tianjin Medical University, Tianjin, China

[6] Department of Respiratory, Tianjin Medical University General Hospital, Tianjin, China

[7] Department of Neurology, School of Medicine, Kaohsiung Medical University, Kaohsiung, Taiwan

[8] Institute of Behavioral Medicine, College of Medicine & Hospital, National Cheng Kung University, Tainan, Taiwan

[9] Department of Psychiatry, National Cheng Kung University, Tainan, Taiwan

inflammation [4]. Bifunctional effects of PGE_2 on inflammatory conditions have been documented. In pathological conditions, PGE_2 regulates multiple processes in the nervous system, including fever generation, sickness behavior, pro-inflammatory cytokines production, such as IL-6 and IL-1β, and also contributes to neuropathic pain and neurodegenerative disorders [5–13]. Conversely, PGE_2 also exhibits anti-inflammatory functions [14, 15]. Several lines of evidence suggest that PGE_2 generated during periods of inflammation is subject to negative feedback in order to downregulate other pro-inflammatory factors [16, 17]. Moreover, accumulating in vivo and in vitro studies reveal that exogenous PGE_2 is able to inhibit lipopolysaccharide (LPS)-induced microglial activation and the production of pro-inflammatory factors, including TNF-α, IL-1β, iNOS, IL-6, and IL12 [18–22].

Numerous studies reveal that PGE_2 displays functionally opposing actions in distinct cell types or disease models, including pro- and anti-inflammatory effects, or toxic and protective effects to neurons [11, 14, 23–27]. The reason for these opposing reports is not clear. We speculated that the difference in concentration of PGE_2 used in various reports could contribute to the controversial conclusions. Most pharmacological studies involve pathological PGE_2 concentrations ranging from 100 nM to 10 μM, which is 100- to 1000-fold higher than physiological concentrations of PGE_2 in the central nervous system (CNS) (< 10 nM), while very few reports use low concentrations of PGE_2 [28–33]. The purpose of this study was to gain a further understanding of the physiological function of PGE_2 in the modulation of brain immune homeostasis by focusing on the effects of sub-nanomolar concentrations of the prostaglandin. In the present study, we investigated whether low concentrations of PGE_2 (0.01 to 10 nM) were capable of eliciting a neuroprotective effect through mediation of pro-inflammatory factors, especially superoxide free radicals produced by the enzyme NADPH oxidase (NOX2), in an LPS-induced neuro-inflammation model. We found that low concentrations of PGE_2 displayed both anti-inflammatory and neuroprotective functions, and further investigation revealed that anti-inflammatory effects were independent of prostaglandin E2 receptors (EP). Additionally, we discovered that inhibition of NOX2-generated superoxide production from microglia was the key mechanism underlying the anti-inflammatory function of sub-nanomolar concentrations of PGE_2.

Materials and Methods

Animals

Timed-pregnant (gestational day 14) female Fisher 344 rats were purchased from Charles River Laboratories (Raleigh, NC, USA). Timed-pregnant C57BL/6J and B6.129S-Cybb<tm1Din>/J (gp91 deficient) mice were generated by our institute's animal husbandry staff using breeders obtained from Jackson Laboratories (Ben Harbor, ME, USA). EP2 knockout mice were kindly gifted from Dr. Robert Langenbach at National Institute of Environmental Health Sciences. Rat and mouse dams were housed in polycarbonate cages in animal facilities with controlled environment conditions with a 12-h artificial light-dark cycle and provided fresh deionized water and NIH 31 chow ad libitum. All animal procedures were approved by the Institutional Animal Care and Use Committee and conducted in strict accordance with the National Institutes of Health animal care and use guidelines.

Reagents

Xanthine, xanthine oxidase, SQ 22,536, L798106, poly-D-lysine, superoxide dismutase (SOD), mazindol, 3,3′-diaminobenzidine, and urea-hydrogen peroxide tablets were purchased from Sigma-Aldrich (St. Louis, MO, USA). Water-soluble tetrazolium salt-1 (WST-1) was purchased from Dojindo (Rockville, MD, USA). Lipopolysaccharide (LPS; *E. coli* strain O111: B4) was purchased from Calbiochem (San Diego, CA, USA). Cell culture ingredients were obtained from Life Technologies (Grand Island, NY, USA). Prostaglandin E_2 (PGE_2), 17-phenyl trinor prostaglandin E_2, butaprost, CAY-10598, SC-19220, AH-6809, and AH-23848 were purchased from Cayman Chemical (Ann Arbor, MI, USA). Anti-tyrosine hydroxylase (TH) was purchased from Chemicon (Billerica, MA, USA) and antibody diluent was purchased from DAKO (Carpinteria, CA, USA). TNF-α ELISA kit was purchased from R&D Systems (Minneapolis, MN, USA). Direct cAMP ELISA kit was purchased from Enzo Life Sciences (Farmingdale, NY, USA). Anti-$p47^{phox}$ antibody was purchased from Millipore (Temecula, CA, USA). Anti-$gp91^{phox}$ antibody was purchased from BD Biosciences (San Jose, CA, USA). Anti-GAPDH antibody was purchased from Abcam (Cambridge, MA, USA). Alexa Fluor 488 goat anti-rabbit IgG was purchased from Invitrogen (Carlsbad, CA, USA). Goat anti-rabbit biotinylated secondary antibody was purchased from Vector Laboratory (Burlingame, CA, USA).

Mesencephalic Neuron-Glia Culture

Rat mesencephalic neuron-glia cultures were prepared following protocols described previously [34, 35]. Briefly, midbrain tissues were dissected from day 14 embryos and then gently triturated into single cell suspension. Cells were then seeded (5×10^5 cells/well) in poly-D-lysine (20 μg/ml) precoated 24-well plates. The cultures were incubated at 37 °C in 5% CO_2 for 3 days and then replenished with 500 μl of fresh maintenance media. Cultures were treated 7 days after seeding.

Primary Cortical Mixed Glial Culture

Primary cortical mixed glial cultures were prepared from rat or mouse pup brains at postnatal days 1–3, as previously described [34, 35]. Briefly, the cortices were isolated, the meninges and blood vessels removed, the tissue gently dissociated through trituration, and the single cell suspension plated on either 24-well plates or 96-well plates precoated in poly-D-lysine (20 μg/ml) at 1×10^5 cells/well or 5×10^4 cells/well, respectively. Cells were maintained in DMEM-F12 (1:1) media supplemented with 10% heat-inactivated fetal bovine serum (FBS), 2 mM L-glutamine, 1 mM sodium pyruvate, 100 μM non-essential amino acids, 50 U/ml penicillin, and 50 μg/ml streptomycin. Media was refreshed every 3 days until they were experimentally treated 7 days after seeding.

Microglia-Enriched Cultures

Microglia-enriched cultures were prepared from primary mixed glial cultures as previously described [34, 35]. Briefly, mixed glia cultures were plated on 150-cm^3 flasks precoated in poly-D-lysine (20 μg/ml) at 5×10^7 cells/flask and were maintained in DMEM-F12 media changed every 3 days for 2 weeks. At 2 weeks, microglia were shaken off at 180 rpm for 40 min and re-plated either on 6-well plates precoated in poly-D-lysine (20 μg/ml) at 1×10^6 cells/well for cAMP assay.

Cell Line Culture

Mycoplasma-free rat HAPI microglial cell line was maintained in DMEM supplemented with 10% FBS, 50 U/ml penicillin, and 50 μg/ml streptomycin. Cells were split into T75 flasks and used for experiments at passages 3–5, where they were seeded in 24-well plates at 1×10^5 cells/well and treated 24 h later.

Wild-type and transfected monkey kidney COS7 cells were gifts from Dr. Mary Dinauer (Indiana University, IN, USA) and cultured as described previously [36, 37]. Briefly, wild-type COS7 cells were grown in DMEM supplemented with 10% fetal bovine serum (FBS), 50 U/ml penicillin, and 50 μg/ml streptomycin. COS7 cells stably expressed with $gp91^{phox}$, $p22^{phox}$, $p47^{phox}$, and $p67^{phox}$ (COS-NOX2 cells) were maintained in DMEM as above containing 0.8 mg/ml Geneticin, 2 μg/ml puromycin, and 0.35 mg/ml hygromycin B.

Dopamine Uptake Assay

The [^{3}H] dopamine (DA) uptake assay was performed as described previously [38]. Briefly, the rate of uptake of radiolabeled DA by DAnergic neuron cultures was measured for 21 min at 37 °C. Cells were washed and lysed to release internalized radiolabeled DA and quantified with a liquid scintillation counter (Tri-Carb 4000; Packard, Meriden, CT, USA). Non-specific [^{3}H] DA uptake was accounted for by competitively inhibiting DA uptake with 10 μM of mazindol.

Immunocytochemical and Immunofluorescence Staining

For immunocytochemical staining, neuron-glia cultures were fixed with 3.7% formaldehyde in phosphate-buffered saline (PBS) for 20 min; fixed cultures were treated with 1% hydrogen peroxide for 10 min and incubated for 20 min with blocking solution (BSA 1%/Triton X-100 0.4%/normal goat serum 4% in PBS). Cells were immunostained overnight at 4 °C with rabbit polyclonal antibody against tyrosine hydroxylase (TH; 1:5000) in Antibody Diluent. Cultures were washed for 10 min in PBS (three times) and incubated for 2 h with PBS containing 0.3% Triton X-100 and a biotinylated secondary antibody (goat anti-rabbit antibody, 1:227; Vector Laboratory, Burlingame, CA). After washing (three times) with PBS, the cultures were incubated for 1 h with the Vectastain ABC reagents (Vector Laboratory, Burlingame, CA) diluted in PBS containing 0.3% Triton X-100. To visualize the signal, the cultures were incubated with 3,3′-diaminobenzidine and urea-hydrogen peroxide tablets dissolved in water. TH-positive cells were manually counted under a microscope (Nikon, model DIAPHOT, Garden City, NY, USA) by at least two investigators and the results were averaged.

For immunofluorescence staining, microglia-enriched cultures were fixed with 3.7% formaldehyde in PBS for 20 min and incubated for 20 min in blocking solution (BSA 1%/Triton X-100 0.4%/normal goat serum 4% in PBS) to block non-specific binding. Cells were immunostained overnight at 4 °C with rabbit polyclonal antibody against p47phox (1:1000) diluted in Antibody Diluent. The antibody was detected and visualized using Alexa Fluor 488 goat anti-rabbit IgG (1:750) secondary antibody. The images were acquired using multiphoton laser-scanning microscope Zeiss 710.

Peritoneal Macrophage Isolation

Macrophages were obtained from peritoneal cavities of mice using protocols described previously [39]. Briefly, mice were injected with 1 ml of 3% Brewer thioglycollate medium into the peritoneal cavity. After 4 days, mice were euthanized, and the peritoneal cavity was flushed with 5 ml ice-cold RPMI medium 1640. After being washed twice in RPMI, the cells were preincubated in the no-serum medium for 1 h. The cells were then washed twice to remove non-adherent cells. Adherent macrophages were cultured in DMEM containing 10% FBS, 50 U/ml penicillin, and 50 μg/ml streptomycin at 37 °C in a humidified atmosphere of 5% CO_2 and 95% air.

[^{3}H]-Labeled PGE_2 Binding Assay

The binding assay was performed according to protocols described previously [40]. Briefly, macrophages from C57BL/6J and CYBB (gp91 deficient) mice, wild-type COS7 cells and COS7 cells stably expressing $gp91^{phox}$, $p47^{phox}$, and $p67^{phox}$ (COS7-NOX2) (2×10^6 cells) were incubated with 0.3 nM of ^{3}H-labeled PGE_2 in binding buffer (HBSS + 10% fetal bovine serum) for 2 h at 37 °C. After binding, the cells were transferred to glass fiber filter with 1 μm pore size and washed three times using warm HBSS. Then the filters were put into vials containing 15 ml of Ultima Gold scintillation fluid (PerkinElmer, Waltham, MA, USA) and counted for radioactivity. The results are expressed as a percentage of total binding observed with corresponding COS7-WT or C57BL/6 group.

Saturation curves of [^{3}H]-PGE_2 binding were performed using COS7-WT and COS7-NOX2 cells. Total binding was measured by the binding of [^{3}H]-labeled PGE_2 ranging from 0.03 to 3 nM while non-specific binding was determined in the presence of additional 3 μM of PGE_2. Specific binding was calculated by the difference between total binding and non-specific binding.

TNF-α, MCP-1, and Nitrite Measurement

The release of TNF-α and MCP-1 was measured from culture supernatant with a commercial enzyme-linked immunosorbent assay (ELISA) kit from R&D Systems, in accordance with the manufacturer's instructions. NO was assessed by measuring nitrite in 50 μl of supernatants using Griess reagent as described previously [41]. The culture supernatant was collect at 3 h after treatment for TNF-α and 24 h after treatment for NO and MCP-1 assay. The results were quantified using an SPECTAmax PLUS 384 spectrophotometer (Molecular Devices, Sunnyvale, CA, USA).

cAMP Assay

Primary microglia cells were seeded in 6-well plates (1×10^6 cells/well) and then treated with vehicle, LPS, or PGE_2 (1, 10, 50, 100, and 1000 nM) for 30 min. Cells were lysed in 0.1 M HCl for 10 min, and the supernatants were used for cAMP assays following the manufacturer's protocol of cAMP Enzyme Immunoassay Kit. The absorbance was measured at 405 nm using a colorimetric 96-well plate reader. Data were expressed as picomoles cAMP per 1 million cells.

Superoxide Assay

The production of extracellular superoxide was determined by measuring the superoxide dismutase (SOD)-inhibitable reduction of water-soluble tetrazolium salt-1 (WST-1) [42, 43]. Mixed glial or neuron-glia cultures in 96-well culture plates were incubated at 37 °C for 30 min with vehicle or PGE_2. Then the cultures were washed twice with HBSS without phenol red. After washing, the cultures were treated with LPS or LPS + PGE_2 in 150 μl phenol red-free, to which 50 μl of WST-1 (1 mM) with and without 800 U/ml SOD was immediately added. The absorbance at 450 nm was read with a SpectraMax Plus microplate spectrophotometer (Molecular Devices, Sunnyvale, CA, USA) and the data at 8–14 min post-treatment were analyzed. The difference in absorbance observed in the presence and absence of SOD was considered to be the amount of superoxide produced, and results were expressed as the percentage of vehicle-treated control cultures. For Fig. 3d, the cultures were pretreated with EP1 to EP4 receptor antagonists for 30 min, and then the steps described above were followed.

Xanthine/Xanthine Oxidase Reaction

Xanthine/xanthine oxidase (X/XO) assays were conducted in the presence of indicated concentrations of PGE_2, 0.01 U xanthine oxidase, 50 μM xanthine, and 250 μM partially acetylated WST-1 in 50 mM potassium phosphate buffer (pH 7.6) in a 96-well plate (100 μl/well final volume). Xanthine was added to initiate the reaction, and the absorbance at 450 nm was continuously monitored for 20 min using an SPECTAmax PLUS 384 spectrophotometer (Molecular Devices, Sunnyvale, CA, USA) and the data at 8–14 min post-treatment were analyzed. Superoxide dismutase (SOD) added in the X/XO system served as a positive control.

Plasma Membrane Preparation and Western Blot Analysis

Plasma membrane of HAPI was isolated following a published protocol [44]. Briefly, cells were suspended in isolation buffer (10 mM Tris–Cl, pH 8.0, 0.25 M sucrose, 1 mM EDTA, and protease inhibitor cocktails), and cell membranes were broken by Dounce homogenization. The cell lysates were centrifuged at 6000×*g* for 10 min at 4 °C to remove unbroken cells, cell debris, and mitochondria; afterward, pellets of membranes were obtained by ultracentrifugation at 100,000×*g* for 1 h at 4 °C. After being washed with 1 M KCl, membrane pellets were either used fresh or stored at − 80 °C. The pellets were solubilized in 1% Nonidet P-40 hypotonic lysis buffer. Equal amounts of protein were separated by 4 to 12% Bis-Tris Nu-PAGE gel and transferred to PVDF membranes (Bio-Rad, Hercules, CA, USA). Membranes were blocked with 5% nonfat milk and incubated with antibodies against $p47^{phox}$, $gp91^{phox}$ (1:1000 dilution), or GAPDH (1:2500 dilution). The protein bands were developed by incubating with horseradish peroxidase-conjugated secondary antibodies (Vector Laboratories, Burlingame, CA, USA) and an enhanced

chemiluminescence substrate kit (Millipore, Billerica, MA, USA). The results were quantified by the AlphaImager 3400 software (Alpha Innotech, Ltd., San Leandro, CA, USA).

Statistics

Data are presented as the mean ± SEM. Comparisons between more than two groups was conducted using one-way ANOVA, followed by Bonferroni's post hoc multiple comparison test. Comparisons between more than two parameters were conducted by two-way ANOVA analysis, followed by Bonferroni's post hoc multiple comparison test. Data were analyzed using Prism (v6.00, GraphPad, San Diego, CA). *P* values less than or equal to 0.05 were considered statistically significant.

Results

Low Nanomolar Concentrations of PGE_2 Protect Dopaminergic Neurons Against LPS-Induced Neurotoxicity

To determine the immune regulatory function of PGE_2 in concentrations close to those found under normal physiological conditions, mesencephalic neuron-glia cultures were pretreated with PGE_2 ranging from 0.01 to 10 nM for 30 min followed by LPS treatment (15 ng/ml). After 7 days, the viability of dopaminergic (DA) neurons was determined by a [^{3}H] DA uptake assay, tyrosine hydroxylase (TH)-positive neuron counting, and morphological analysis. [^{3}H] DA uptake showed that pretreatment of PGE_2 protected neurons against LPS-induced neurotoxicity ($F_{(5, 33)} = 30$, $P < 0.0001$) in a dose-dependent manner. Post hoc analysis revealed that exposure of LPS reduced DA uptake capacity by 60% compared to vehicle-treated cultures ($t = 11.1$, $P < 0.0001$). Pretreatment with PGE_2 significantly blocked this reduction at 1 nM ($t = 5.028$, $P < 0.0001$) and 10 nM ($t = 7.022$, $P < 0.0001$), when compared to DA uptake in LPS-only treatments (Fig. 1a). Consistent with DA uptake results, TH-positive neuron count showed a similar protective effect of PGE_2 ($F_{(5, 36)} = 11.2$, $P < 0.0001$) (Fig. 1b). Post hoc analysis showed that neuroprotective effects of PGE_2 were observed in concentrations as low as 0.1 nM (0.1 nM: $t = 3.245$, $P < 0.05$; 1 nM: $t = 4.275$, $P < 0.01$; 10 nM: $t = 4.838$, $P < 0.001$), compared to the LPS-only treatments. Morphological analysis showed that the neurites of TH-positive neurons in LPS-treated cultures were short and fragmented compared to those in the control cultures. The neurites in cultures pretreated with PGE_2 were less affected, compared with neurites in LPS-treated cultures (Fig. 1c). Together, these results indicate that nanomolar concentrations of PGE_2 exert potent neuroprotective effects against LPS-induced neurotoxicity.

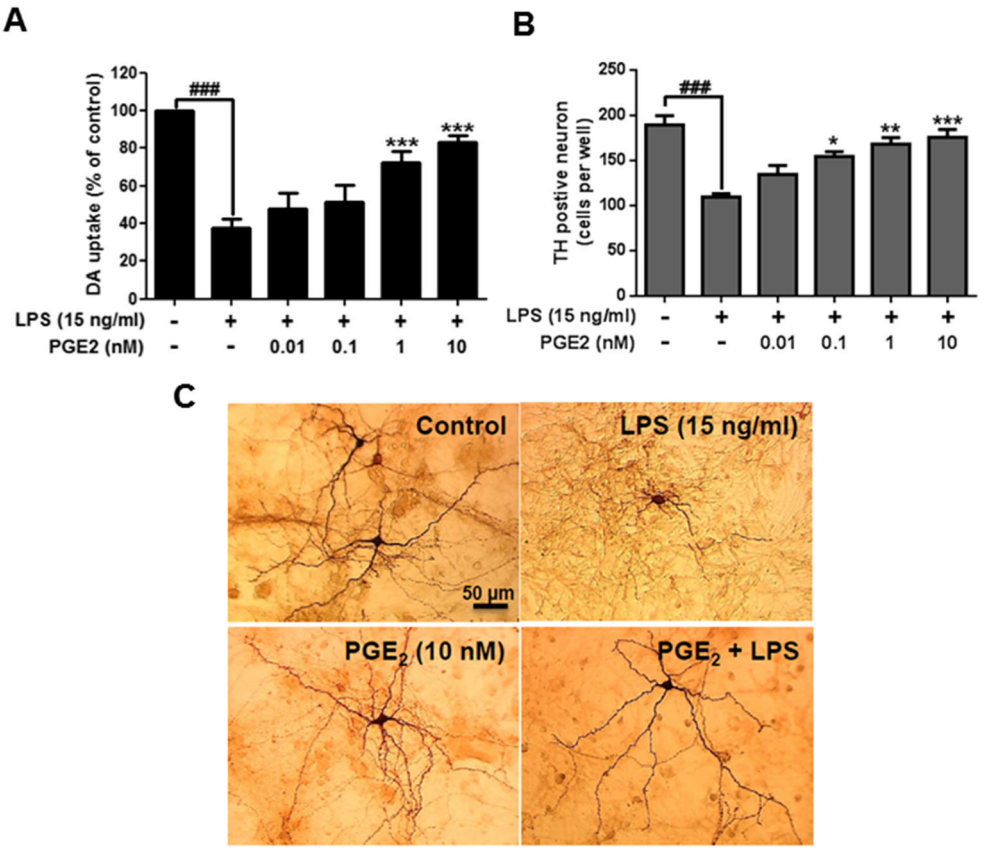

Fig. 1 Reduction of LPS-induced dopamine neuron toxicity in midbrain neuron-glia cultures after 7 days, as seen by **a** [^{3}H] DA uptake, **b** TH-positive neuron count, and **c** immunostaining. Scale bar, 50 µm. Primary rat midbrain neuron-glia cultures were pretreated with PGE_2 for 30 min followed by LPS treatment (15 ng/ml). Values are mean ± SEM from three independent experiments, with duplicates for each experiment. Data were analyzed with one-way ANOVA followed by Bonferroni's post hoc multiple comparison test. $^*P < 0.05$, $^{**}P < 0.01$, $^{###}$, $^{***}P < 0.0001$ Bonferroni's *t* test compared to vehicle-treated group and LPS-treated group, respectively

PGE_2 Displays Varying Potency in Inhibiting LPS-Induced Production of Pro-inflammatory Factors in Mixed Glial Cultures

Accumulating evidence indicates that neuro-inflammation caused by over-activated microglia is a critical contributor to neuronal loss in neuro-degeneration. Our previous primary neuron-glia culture studies indicate that microglia are the major source of LPS-stimulated production of pro-inflammatory factors (e.g., cytokines, chemokines, and free radicals), which mediate neuro-inflammation and cause neurotoxicity [8]. To investigate the mechanisms of neuroprotection elicited by nanomolar concentrations of PGE_2, we investigated the release of pro-inflammatory factors in rat mixed glial cultures (containing 80% astroglia and 20% microglia). The reason why mixed glia cultures were used in lieu of enriched microglia cultures in this study was microglia can survive longer when cultured together with either neurons or astroglia [45, 46]. The results revealed that PGE_2 reduced the production of superoxide, TNF-α, NO, and MCP-1 (superoxide, $F_{(5,\ 18)} = 69.35$, $P < 0.0001$; TNF-α, $F_{(7,\ 79)} = 340.8$, $P < 0.0001$; NO, $F_{(7,\ 67)} = 55.78$, $P < 0.0001$; MCP-1, $F_{(5,\ 12)} = 34.87$, $P < 0.0001$) in a dose-dependent manner (Fig. 2). However, it is interesting to note that the inhibitory potency of PGE_2 varies greatly: the half-maximal inhibitory concentration (IC_{50}) value is 0.13 ± 0.08 nM for inhibition of superoxide, 10.14 ± 0.18 nM for TNF-α, and more than 100 nM for both NO and MCP-1 production. These results suggest that PGE_2 inhibited production of these pro-inflammatory factors through different mechanisms. Moreover, the similar IC_{50} values of PGE_2 in inhibiting neurotoxicity (0.14 nM) and superoxide production (0.13 nM) suggest a strong likelihood that the inhibition of superoxide production is critical in mediating PGE_2-elicited neuroprotective effects. Thus, more detailed studies were conducted to further understand the molecular mechanisms underlying the regulation of superoxide production by nanomolar concentrations of PGE_2.

Inhibition of Superoxide Production Is Not Due To the Scavenging Effect of PGE_2 and Is Not Mediated Through EP Receptors

One of the mechanisms of suppressing superoxide production is scavenging of superoxide by agents of interest. To investigate this possibility, we determined whether nanomolar concentrations of PGE_2 possess the ability to scavenge superoxide free radicals. We measured the effect of PGE_2 on superoxide production using a xanthine/xanthine oxidase superoxide-producing system. Superoxide production was dramatically inhibited by superoxide dismutase (SOD), but not by PGE_2 with different concentrations (0.01–10 nM) (Supplementary Fig. 1).

The lack of a superoxide-scavenging effect of PGE_2 prompted us to investigate the potential signaling pathway mediating the inhibitory effects of PGE_2 on superoxide production. Using a pharmacological approach, we determined the potency of different agonists selective for EP receptor subtypes in inhibiting LPS-induced superoxide production.

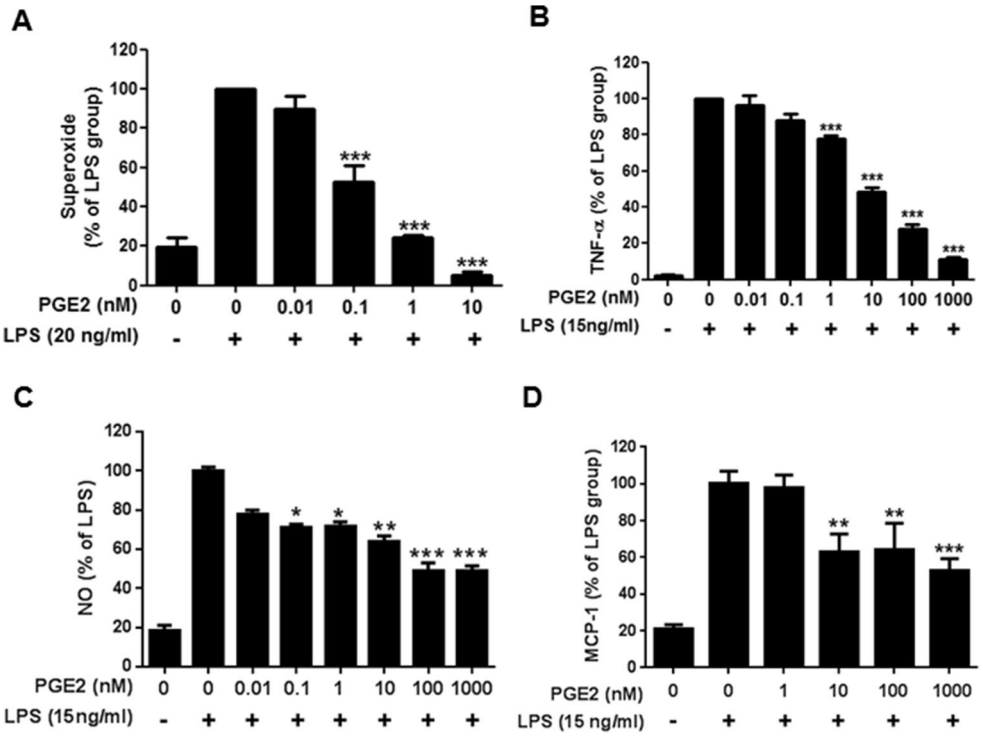

Fig. 2 Dose-dependent inhibitory effects of PGE2 on LPS-stimulated production of pro-inflammatory factors **a** superoxide, **b** TNF-α, **c** NO, and **d** MCP-1 with different IC_{50} values. Rat mixed glia cultures were pretreated with various concentrations of PGE_2 for 30 min followed by LPS treatment. Values are mean ± SEM from three independent experiments, with duplicates for each experiment. $^*P < 0.05$, $^{**}P < 0.01$, $^{***}P < 0.0001$ Bonferroni's *t* test compared to LPS-only group

Rat mixed glial cultures were pretreated with various agonists, 17-phenyltrinor PGE_2 (EP1/3 agonist), butaprost (EP2 agonist), and CAY10598 (EP4 agonist) with concentrations ranging from 0.01 to 10 nM for 30 min prior to LPS (20 ng/ml) stimulation. The results showed that all EP agonists mimicked the inhibitory effects of PGE_2 on superoxide production, with IC_{50} values similar to that of PGE_2 (17-phenyl trinor PGE_2, $F_{(5,\ 12)} = 60.07$, $P < 0.0001$; butaprost, $F_{(5,\ 24)} = 187.9$, $P < 0.0001$; CAY10598, $F_{(5,\ 12)} = 37.93$, $P < 0.0001$) (Fig. 3a–c). Moreover, simultaneously blocking all four EP receptors by adding receptor antagonists to mixed glial cultures failed to disrupt the inhibitory effect of PGE_2 (Fig. 3d). The EP receptor-independent effect of PGE_2 was further supported by using EP receptor-deficient mixed glial cultures. Here, we used mixed glial cultures prepared from EP2 receptor knockout mice because the EP2 receptor has been previously implicated to be critical in mediating the anti-inflammatory effect of micromolar concentrations of PGE_2 [47–49]. PGE_2-induced inhibition of superoxide production did not differ between EP2-deficient and control mixed glia cultures, indicating that the EP2 receptor was not involved in mediating nanomolar PGE_2-induced inhibition of superoxide (Fig. 3e). Additionally, the EP2 receptor agonist butaprost was still capable of inhibiting superoxide production in EP2-deficient mixed glia cultures (Fig. 3f). Since different signaling pathways mediate each EP receptor subtype and cause distinct cellular effects [3], the similar potencies displayed by these EP receptor agonists suggest that their inhibitory properties may be mediated by a novel, EP receptor-independent mechanism. Taken together, these results demonstrate that

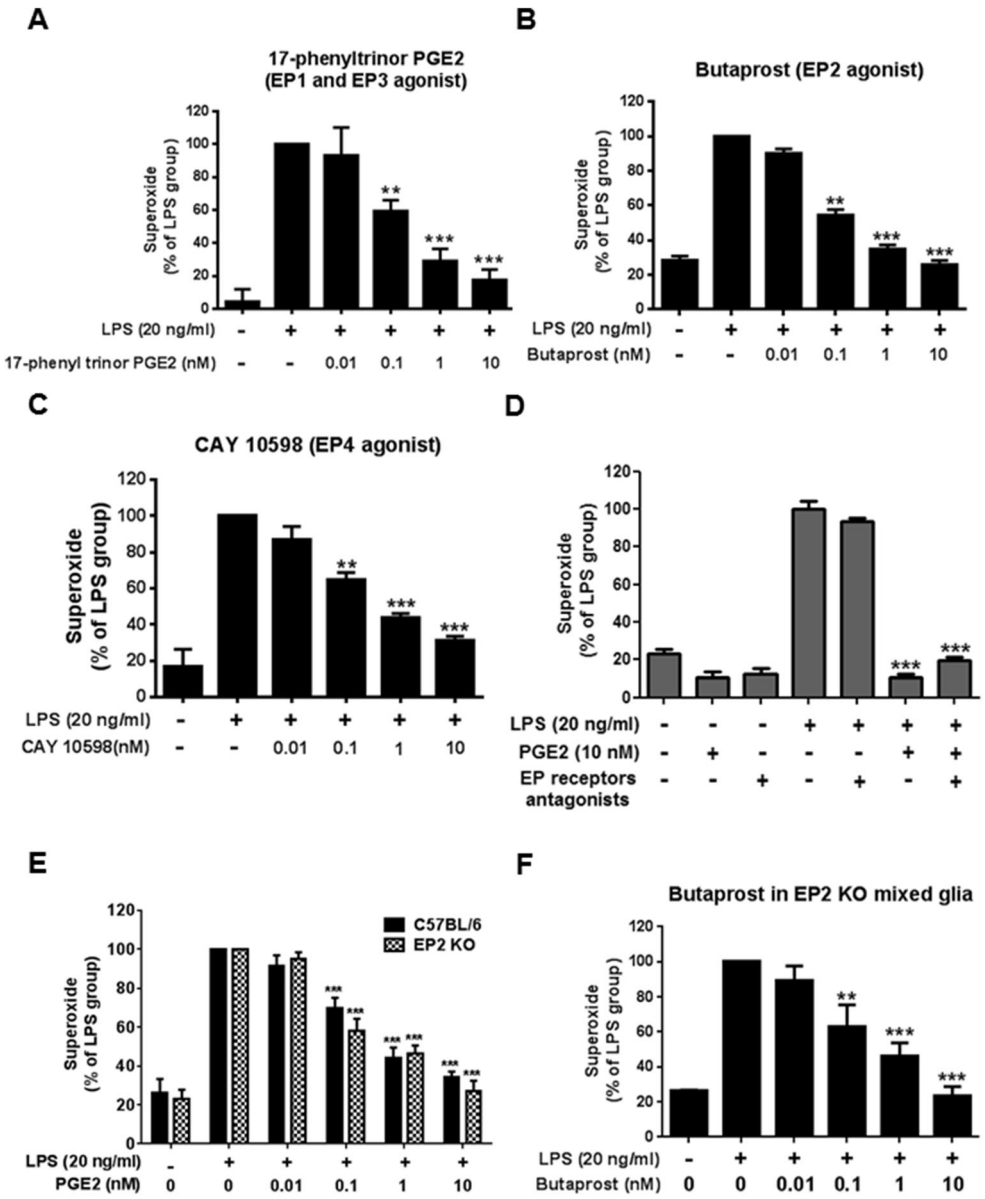

Fig. 3 Rat mixed glia cultures were pretreated with various concentrations of **a** 17-phenyltrinor PGE_2, **b** butaprost, and **c** CAY10598 for 30 min and then exposed to 20 ng/ml of LPS. **d** Rat mixed glia cultures were pretreated with a combination of 4 EP receptor subtype antagonists, SC-19220 (EP1, 3 μM), AH-6809 (EP2, 3 μM), L-798106 (EP3, 1 μM), and AH-23848 (EP4, 1 μM), for 30 min, followed by 10 nM of PGE_2 for additional 30 min, and then exposed to 20 ng/ml of LPS. **e** Wild-type (C57BL/6) and EP2 receptor KO mixed glia cultures were treated with various concentrations of PGE_2 for 30 min and then exposed to 20 ng/ml of LPS. **f** EP2 receptor KO mixed glia cultures were treated with various concentrations of butaprost for 30 min and then exposed to 20 ng/ml of LPS. The generation of superoxide was measured by monitoring the SOD-inhibitable reduction of WST-1. Values are mean ± SEM from four independent experiments, with duplicates. $^{**}P < 0.01$, $^{***}P < 0.0001$ Bonferroni's *t* test compared to LPS-only group

inhibition of LPS-induced superoxide is not due to the superoxide-scavenging capacity of PGE_2 at low concentrations and is instead mediated through a novel EP receptor-independent mechanism.

NOX2 Plays a Pivotal Role in the Neuroprotective Effects of Low Concentrations of PGE_2

As a key superoxide-producing enzyme in activated phagocytes such as microglia, NADPH oxidase (NOX2) is composed of two membrane subunits ($gp91^{phox}$ and $p22^{phox}$) and several cytosolic subunits ($p47^{phox}$, $p67^{phox}$, $p40^{phox}$, Rac1, and Rap1A). Previous reports indicate that activation of microglial NOX2 is key to the pathogenesis of inflammation-related neuro-degeneration, and its $gp91^{phox}$ subunit is a target for several anti-inflammatory agents [50, 51]. To further investigate whether the neuroprotective effect of low doses of PGE_2 is mediated through NOX2, we determined the viability of DA neurons in both wild-type and NOX2-deficient neuron-glial cultures. Genetic ablation of $gp91^{phox}$ abolished neuroprotection by PGE_2 (Fig. 4), indicating that NOX2 plays a critical role in mediating the anti-inflammatory and neuroprotective effects of low concentrations of PGE_2.

PGE_2 Directly Interacts with NADPH Oxidase Subunit $gp91^{phox}$

To investigate the possibility that PGE_2 suppressed LPS-induced superoxide production by inhibiting NOX2 through binding to the $gp91^{phox}$ subunit, we conducted a binding assay using tritium labeled PGE_2. We compared the binding capacity of PGE_2 in wild-type COS7 cells and COS7 cells transfected with NOX2 membrane subunits ($gp91^{phox}$/$p22^{phox}$) and cytosolic subunits ($p47^{phox}$ and $p67^{phox}$) (COS7-NOX2). The reason for the co-transfection of $gp91^{phox}$ and $p22^{phox}$ is that $p22^{phox}$ facilitates stable expression of $gp91^{phox}$ in the plasma membrane of COS7 cells [52]. The [^{3}H]-labeled PGE_2 binding assay showed that COS7-NOX2 cells have a binding capacity to [^{3}H]-PGE_2 that is 2-fold higher than that of wild-type COS7 cells ($P < 0.0001$, Fig. 5a). We also compared the PGE_2 binding capacity in macrophages isolated from wild-type and $gp91^{phox-/-}$ mice. We used peritoneal macrophages instead of microglia in this study for the following reasons: (1) microglia are considered to be the macrophages of the brain, as both cells are derived from bone marrow monocytes, and the protein structure of $gp91^{phox}$ of these two cell types is identical; (2) macrophages have high levels of $gp91^{phox}$, and it was easy to generate large numbers of primary macrophages required for this study. The [^{3}H]-PGE_2 binding capacity was significantly reduced in macrophages from $gp91^{phox-/-}$ mice than in that from wild-type mice ($P < 0.01$, Fig. 5b). The saturation study was performed

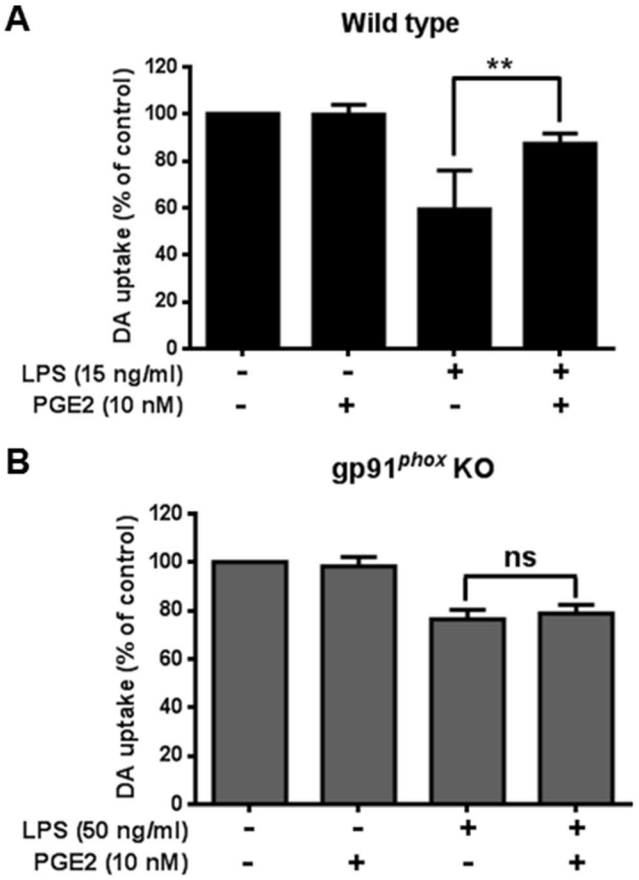

Fig. 4 Midbrain neuron-glia cultures from **a** wild-type and **b** $gp91^{phox}$ KO mice were pretreated with PGE_2 (10 nM) for 30 min and then exposed to LPS (15 ng/ml). After 7 days, the cultures were subjected to DA uptake assay. Values are mean ± SEM from three independent experiments, with triplicates. $^{**}P < 0.01$, Bonferroni's *t* test compared to LPS-only group

using wild-type COS7-WT and transfected COS7-NOX2 cells. The [^{3}H]-PGE_2 binding was saturable with a binding affinity at a low nanomolar concentration range (Fig. 5c, d). The calculated K_d value was 0.83 ± 0.04 nM, which is close to the IC_{50} concentrations for the inhibition of both LPS-induced superoxide production (0.13 nM) and neurotoxicity (0.14 nM). These results give credence to the possibility that PGE_2 inhibits LPS-induced superoxide production and subsequent neurotoxicity by binding to the $gp91^{phox}$ subunit.

PGE_2 Inhibits the LPS-Induced Increase in Translocation of the Cytosolic Subunit $p47^{phox}$ to the Cell Membrane

The activation of NOX2 requires the translocation of phosphorylated cytosolic subunits ($p47^{phox}$, $p67^{phox}$, and $p40^{phox}$) to the cell membrane to form the active enzyme complex by binding to the membrane subunits $gp91^{phox}$ and $p22^{phox}$. We previously reported that several anti-inflammatory agents reduced the production of superoxide by changing the

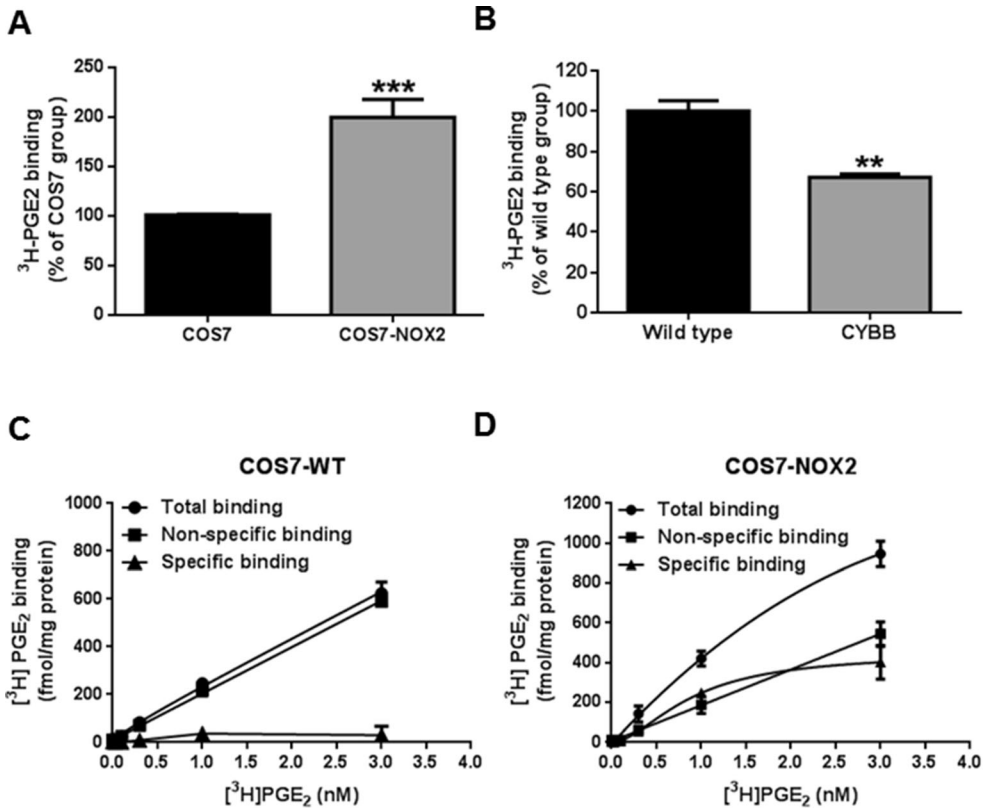

Fig. 5 **a** Wild-type COS7 cells and COS7 cells stably expressing gp91^{phox} and p22^{phox}, p47^{phox} and p67^{phox} (COS7-NOX2) cells were used to conduct the [^{3}H]-labeled PGE$_2$ binding assay. **b** Wild-type (gp91$^{phox+/+}$) and gp91^{phox}-deficient (CYBB) macrophages were used to conduct the [^{3}H]-labeled PGE$_2$ binding assay. Data are shown as a percentage of the wild-type control. Results are presented as means ± SEM from three independent experiments in duplicate. ***$P < 0.0001$ and **$P < 0.01$, paired t test. Saturation curves of [^{3}H]-PGE$_2$ binding were conducted using COS7-WT (**c**) and COS7-NOX2 cells (**d**). Total binding was measured by the binding of [^{3}H]-labeled PGE$_2$ ranging from 0.03 to 3 nM while non-specific binding was determined in the presence of additional 3 μM of PGE$_2$. Saturation isotherms were analyzed in GraphPad Prism 6. Specific binding was calculated by the difference between total binding and non-specific binding. This experiment was conducted three times with similar results

conformation of the membrane subunit gp91^{phox} to reduce the binding affinity for the cytosolic subunits of NOX2 and prevent their translocation to the membrane [51]. To obtain additional evidence supporting the possibility that NOX2 acts through a novel signaling pathway that mediates the anti-inflammatory action of PGE$_2$, we examined the membrane translocation of the cytosolic subunit p47^{phox} by determining the level of p47^{phox} in cytosol and membrane. Primary microglia were pretreated with/without 10 nM of PGE$_2$ for 30 min following by LPS stimulation for 15 min. Staining results showed that LPS significantly increased the immunofluorescence intensity in the membrane, indicating translocation of the cytosolic subunit p47^{phox} to the membrane. Pretreatment with PGE$_2$ alone did not differ from the control while when combined with LPS, it almost completely prevented the LPS-induced translocation of p47^{phox} to the membrane (Fig. 6a). We also conducted Western blot analysis to verify the result of immunofluorescence staining. In this study, rat microglia cell line HAPI cells were used, due to the large number of high purity cells of this type that can be harvested for Western blot analysis. Consistent with immunostaining results, LPS stimulation significantly increased the band intensity of p47^{phox} in the membrane fraction (control vs. LPS, $t = 10.86$, $P < 0.001$). PGE$_2$ pretreatment completely prevented these changes (LPS vs. PGE$_2$ + LPS, $t = 10.47$, $P < 0.001$) (Fig. 6b, c). Taken together, these results suggest that PGE$_2$ can bind to the subunit of NOX2 gp91^{phox} to inhibit the LPS-induced translocation of cytosolic p47^{phox} and subsequent superoxide production.

Discussion

The anti-inflammatory effects of PGE$_2$ have been extensively studied under both pharmacological and pathological conditions. However, concentrations of PGE$_2$ used in such studies are in the micromolar range (0.1–10 μM) and are rarely observed under normal physiological conditions. The present study demonstrated that low concentrations of PGE$_2$ (0.01 to 10 nM), which are close to normal brain extracellular concentrations (< 10 nM) [28–33], exert potent protection of LPS-induced DA neuron damage via a reduction in the release of

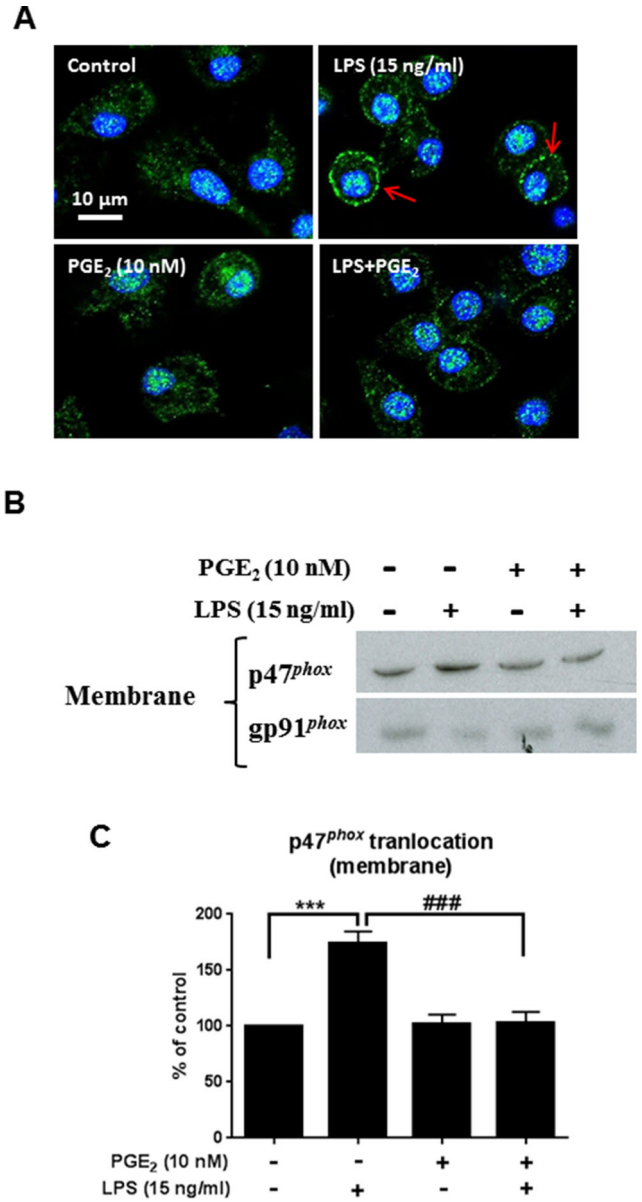

Fig. 6 **a** Primary microglial cells were pretreated with PGE_2 or vehicle for 30 min and then stimulated with LPS (15 ng/ml) for 15 min. Cells were immunostained with a rabbit polyclonal antibody against $p47^{phox}$ (green) and DAPI (blue). Scale bar, 10 μm. **b**, **c** HAPI cells (rat microglia cell line) were pretreated with PGE_2 (10 nM) or vehicle for 30 min, followed by LPS stimulation (15 ng/ml). After LPS stimulation for 15 min, subcellular fractions were isolated to conduct Western blot analysis in order to determine the level of $p47^{phox}$ in the membrane fractions. $gp91^{phox}$ was used as membrane internal control. Values are mean ± SEM from three independent experiments. $^{***}P < 0.0001$ Bonferroni's *t* test compared to vehicle-treated group; $^{\#\#\#}P < 0.0001$ Bonferroni's *t* test compared to LPS-treated group

pro-inflammatory factors, especially the release of reactive oxygen species (ROS) from microglia. Further, the mechanistic studies conducted here reveal that the anti-inflammatory and neuroprotective effects of low concentrations of PGE_2 are not mediated through the conventional EP receptors (EP1-EP4). Instead, we found that PGE_2 could directly inhibit the activation of microglial NOX2 by binding to its catalytic membrane subunit $gp91^{phox}$. Our study also indicates that a reduction in superoxide production plays a major role in PGE_2-induced anti-inflammatory neuroprotective effects. These findings revealed a receptor-independent novel mechanism by which physiological concentrations of PGE_2 function to maintain brain immune homeostasis.

PGE_2 has been reported to exert both pro- and anti-inflammatory effects; however, the reasons behind these opposing effects remain unclear. Use of different concentrations and experimental models could be responsible for some of these bifunctional effects of PGE_2. We hypothesized that the difference in concentrations could play a role in these opposite effects of PGE_2 on immune function. Therefore, this study focused on elucidating the mechanism(s) mediating the action of PGE_2 in low concentrations. The LPS-induced release of pro-inflammatory factors, including TNF-α, MCP-1, nitric oxide, and superoxide-related ROS from microglia, was found to decline in the presence of PGE_2 in a dose-dependent manner. However, the IC_{50} concentrations of PGE_2 necessary to suppress these pro-inflammatory factors varied greatly. Among these immune factors, superoxide production was the most critical factor related to the anti-inflammatory and neuroprotective effects of PGE_2; 1.0 nM of PGE_2 completely suppressed LPS-induced production of superoxide and achieved total neuroprotection. In contrast, higher concentrations of PGE_2 were needed to inhibit LPS-induced production of TNF-α, MCP-1, and nitric oxide to exert a neuroprotective effect. These findings prompted us to search in further detail for the mechanism(s) behind inhibition of superoxide production in the presence of low concentrations of PGE_2.

The most salient finding of this study is the EP receptor-independent inhibition of superoxide production by low concentrations of PGE_2. Most of our knowledge regarding the inhibition of superoxide production by PGE_2 arrived from studies on peripheral phagocytes using micromolar concentrations of PGE_2 [47–49], which indicate that the EP2/cAMP signaling pathway plays a pivotal role in inhibition of superoxide production inhibition by PGE_2. In contrast, the lack of suppression of superoxide by either low concentrations of PGE_2 or the EP2 agonist butaprost in EP2 receptor-deficient mixed glia cultures, along with a lack of effect of combined pretreatment with EP1-4 receptor antagonists on PGE_2-induced inhibition of superoxide, implies the existence of an EP receptor-independent regulatory mechanism in superoxide inhibition by PGE_2 in microglia. Moreover, we found that cAMP was undetectable in primary microglial cells treated with 10 nM or less of PGE_2 (Supplementary Fig. 2), further supporting the EP receptor-independent effect of PGE_2.

Previous studies have shown that NOX2, the main superoxide-producing enzyme on microglia cell membranes, is an important source of ROS [50, 53, 54]. ROS, including the superoxide anion, hydroxyl radical, lipid hydroperoxides,

and hydrogen peroxide, are generated from activated microglia and play important roles in amplifying the expression of pro-inflammatory genes in microglia and subsequent neurodegeneration [53]. Various in vitro and in vivo studies indicate that deficiency in NOX2 or pharmacological inhibition of this enzyme's activity can significantly reduce the production of pro-inflammatory factors, as well as subsequent neurodegeneration [50, 55, 56]. Such studies prompted us to speculate that NOX2 could be the target of physiological concentrations of PGE_2, and the following evidence strongly supports this hypothesis: (1) all the specific agonists for the different EP receptor subtypes, such as 17-phenyltrinor PGE2 (EP1 and EP3), butaprost (EP2) and CAY10598 (EP4), displayed similar potencies as PGE_2 in inhibiting superoxide production (Figs. 2a and 3a–c). In contrast, EP receptor antagonists or lack of an EP2 receptor failed to influence the inhibitory effects of PGE_2. These results further indicate that a superoxide-generating enzyme, rather than any of the EP receptors, is a common target for the different PGE_2 analogs. (2) The ligand binding studies indicated that PGE_2 bound to the membrane catalytic subunit $gp91^{phox}$ with a high affinity (i.e., a K_d value around 10^{-10} M), which is close to the K_i value for inhibition of superoxide production (Fig. 5c, d). (3) PGE_2 failed to reduce superoxide produced by the xanthine/xanthine oxidase system, indicating that the inhibition of superoxide production by PGE_2 is not due to its superoxide free radical-scavenging effect (Supplementary Fig. 1). Together, the evidence indicates that NOX2 is a novel target mediating the anti-inflammatory action of nanomolar concentrations of PGE_2.

To further understand the nature how PGE_2 interacts with the catalytic subunit $gp91^{phox}$, we conducted a pharmacophore analysis by comparing PGE_2 with a series of conventional NOX2 inhibitors. Despite the differences in chemical structures between PGE_2 and its analogs used in this study and some of the known NOX2 inhibitors (e.g., diphenyleneiodonium (DPI), apocynin, or naloxone [51]), the analysis showed that several chemical features shared between PGE_2, EP receptor agonists, and NOX2 inhibitors, as deduced by the program Molecular Operating Environment (MOE, Chemical Computing Group, Inc., Montreal, Canada), include hydrophobic centroids, hydrogen bond acceptors, and hydrogen bond donors (Supplementary Fig. 3). Thus, it is likely that PGE_2 and EP receptor agonists might share similar binding properties to microglial NOX2 as DPI and naloxone, hence eliciting similar biological effects.

Although we have identified microglial $gp91^{phox}$ as a novel binding site for PGE_2 in eliciting its anti-inflammatory effect, the underlying mechanism(s) into how PGE_2 inhibits NOX2 activation remains to be determined. Our previous study indicated that after binding, the NOX2 inhibitor, may alter the conformation of $gp91^{phox}$ and hinder the binding of cytosolic subunits, including $p67^{phox}$ and $p47^{phox}$, thus preventing formation of an active enzyme complex [51]. Since the crystal structure of $gp91^{phox}$ is still unavailable, we were not able to demonstrate this actual conformational change after treatment with PGE_2. Thus, we used an alternative approach by determining the translocation of cytosolic subunits to the cell membrane and demonstrated that PGE_2 reduces the translocation of $p47^{phox}$ to the cell membrane (Fig. 6).

In summary, this study demonstrated that physiological concentrations of PGE_2 elicited potent anti-inflammatory/neuroprotective effects. These actions are mediated through a novel EP receptor-independent mechanism by inhibiting activation of microglial NOX2 via direct binding to its catalytic subunit $gp91^{phox}$. These results provide new insights into the potential physiological function of PGE_2 in maintaining CNS immune homeostasis.

Acknowledgements This research was supported by the Intramural Research Program of the NIH, National Institute of Environmental Health Sciences. We thank Drs. Jerry Liu, Hong Li, Peter Egeghy, and David Herr for the critical reading of the manuscript. We thank the animal care team members, Anthony Lockhart, Katrina Loper, and Johnny Green and the members of Fluorescence Microscopy and Imaging Center, Charles J. Tucker and Agnes Janoshazi. The US Environmental Protection Agency has provided administrative review and has approved this paper for publication. The views expressed in this paper are those of the authors and do not necessarily reflect the views of the US Environmental Protection Agency.

Compliance with Ethical Standards

Conflict of Interest The authors declare that they have no conflict of interest.

References

1. Kalinski P (2012) Regulation of immune responses by prostaglandin E2. J Immunol 188(1):21–28. https://doi.org/10.4049/jimmunol.1101029
2. O'Banion MK (2010) Prostaglandin E2 synthases in neurologic homeostasis and disease. Prostaglandins Other Lipid Mediat 91(3–4):113–117. https://doi.org/10.1016/j.prostaglandins.2009.04.008
3. Harris SG, Padilla J, Koumas L, Ray D, Phipps RP (2002) Prostaglandins as modulators of immunity. Trends Immunol 23(3):144–150
4. Minghetti L, Levi G (1998) Microglia as effector cells in brain damage and repair: focus on prostanoids and nitric oxide. Prog Neurobiol 54(1):99–125
5. Saper CB, Romanovsky AA, Scammell TE (2012) Neural circuitry engaged by prostaglandins during the sickness syndrome. Nat Neurosci 15(8):1088–1095. https://doi.org/10.1038/nn.3159
6. Cimino PJ, Keene CD, Breyer RM, Montine KS, Montine TJ (2008) Therapeutic targets in prostaglandin E2 signaling for neurologic disease. Curr Med Chem 15(19):1863–1869
7. Feng ZH, Wang TG, Li DD, Fung P, Wilson BC, Liu B, Ali SF, Langenbach R et al (2002) Cyclooxygenase-2-deficient mice are resistant to 1-methyl-4-phenyl1, 2, 3, 6-tetrahydropyridine-induced damage of dopaminergic neurons in the substantia nigra. Neurosci Lett 329(3):354–358

8. Block ML, Zecca L, Hong JS (2007) Microglia-mediated neurotoxicity: uncovering the molecular mechanisms. Nat Rev Neurosci 8(1):57–69. https://doi.org/10.1038/nrn2038
9. McGeer PL, McGeer EG (2004) Inflammation and neurodegeneration in Parkinson's disease. Parkinsonism Relat Disord 10(Suppl 1):S3–S7
10. Kunori S, Matsumura S, Okuda-Ashitaka E, Katano T, Audoly LP, Urade Y, Ito S (2011) A novel role of prostaglandin E2 in neuropathic pain: blockade of microglial migration in the spinal cord. Glia 59(2):208–218. https://doi.org/10.1002/glia.21090
11. Liang X, Wang Q, Shi J, Lokteva L, Breyer RM, Montine TJ, Andreasson K (2008) The prostaglandin E2 EP2 receptor accelerates disease progression and inflammation in a model of amyotrophic lateral sclerosis. Ann Neurol 64(3):304–314. https://doi.org/10.1002/ana.21437
12. Jiang J, Dingledine R (2013) Prostaglandin receptor EP2 in the crosshairs of anti-inflammation, anti-cancer, and neuroprotection. Trends Pharmacol Sci 34(7):413–423. https://doi.org/10.1016/j.tips.2013.05.003
13. Quan Y, Jiang J, Dingledine R (2013) EP2 receptor signaling pathways regulate classical activation of microglia. J Biol Chem 288(13):9293–9302. https://doi.org/10.1074/jbc.M113.455816
14. Milatovic D, Montine TJ, Aschner M (2011) Prostanoid signaling: dual role for prostaglandin E2 in neurotoxicity. Neurotoxicology 32(3):312–319. https://doi.org/10.1016/j.neuro.2011.02.004
15. Scher JU, Pillinger MH (2009) The anti-inflammatory effects of prostaglandins. J Investig Med 57(6):703–708. https://doi.org/10.2310/JIM.0b013e31819aaa76
16. Kandil HM, Argenzio RA, Sartor RB (1999) Low endogenous prostaglandin E2 predisposes to relapsing inflammation in experimental rat enterocolitis. Dig Dis Sci 44(10):2110–2118
17. Harizi H, Juzan M, Grosset C, Rashedi M, Gualde N (2001) Dendritic cells issued in vitro from bone marrow produce PGE(2) that contributes to the immunomodulation induced by antigen-presenting cells. Cell Immunol 209(1):19–28. https://doi.org/10.1006/cimm.2001.1785
18. Zhang J, Rivest S (2001) Anti-inflammatory effects of prostaglandin E2 in the central nervous system in response to brain injury and circulating lipopolysaccharide. J Neurochem 76(3):855–864
19. Caggiano AO, Kraig RP (1999) Prostaglandin E receptor subtypes in cultured rat microglia and their role in reducing lipopolysaccharide-induced interleukin-1beta production. J Neurochem 72(2):565–575
20. Minghetti L, Nicolini A, Polazzi E, Creminon C, Maclouf J, Levi G (1997) Inducible nitric oxide synthase expression in activated rat microglial cultures is downregulated by exogenous prostaglandin E2 and by cyclooxygenase inhibitors. Glia 19(2):152–160
21. Petrova TV, Akama KT, Van Eldik LJ (1999) Selective modulation of BV-2 microglial activation by prostaglandin E(2). Differential effects on endotoxin-stimulated cytokine induction. J Biol Chem 274(40):28823–28827
22. Aloisi F, Penna G, Cerase J, Menendez Iglesias B, Adorini L (1997) IL-12 production by central nervous system microglia is inhibited by astrocytes. J Immunol 159(4):1604–1612
23. Montine TJ, Milatovic D, Gupta RC, Valyi-Nagy T, Morrow JD, Breyer RM (2002) Neuronal oxidative damage from activated innate immunity is EP2 receptor-dependent. J Neurochem 83(2):463–470
24. Liang X, Wang Q, Hand T, Wu L, Breyer RM, Montine TJ, Andreasson K (2005) Deletion of the prostaglandin E2 EP2 receptor reduces oxidative damage and amyloid burden in a model of Alzheimer's disease. J Neurosci 25(44):10180–10187. https://doi.org/10.1523/JNEUROSCI.3591-05.2005
25. Bilak M, Wu L, Wang Q, Haughey N, Conant K, St Hillaire C, Andreasson K (2004) PGE2 receptors rescue motor neurons in a model of amyotrophic lateral sclerosis. Ann Neurol 56(2):240–248. https://doi.org/10.1002/ana.20179
26. Andreasson K (2010) Emerging roles of PGE2 receptors in models of neurological disease. Prostaglandins Other Lipid Mediat 91(3–4):104–112. https://doi.org/10.1016/j.prostaglandins.2009.04.003
27. Jiang J, Quan Y, Ganesh T, Pouliot WA, Dudek FE, Dingledine R (2013) Inhibition of the prostaglandin receptor EP2 following status epilepticus reduces delayed mortality and brain inflammation. Proc Natl Acad Sci U S A 110(9):3591–3596. https://doi.org/10.1073/pnas.1218498110
28. Ciceri P, Zhang Y, Shaffer AF, Leahy KM, Woerner MB, Smith WG, Seibert K, Isakson PC (2002) Pharmacology of celecoxib in rat brain after kainate administration. J Pharmacol Exp Ther 302(3):846–852
29. Golovko MY, Murphy EJ (2008) An improved LC-MS/MS procedure for brain prostanoid analysis using brain fixation with head-focused microwave irradiation and liquid-liquid extraction. J Lipid Res 49(4):893–902. https://doi.org/10.1194/jlr.D700030-JLR200
30. Sapirstein A, Saito H, Texel SJ, Samad TA, O'Leary E, Bonventre JV (2005) Cytosolic phospholipase A2alpha regulates induction of brain cyclooxygenase-2 in a mouse model of inflammation. Am J Physiol Regul Integr Comp Physiol 288(6):R1774–R1782. https://doi.org/10.1152/ajpregu.00815.2004
31. Loh JK, Hwang SL, Lieu AS, Huang TY, Howng SL (2002) The alteration of prostaglandin E2 levels in patients with brain tumors before and after tumor removal. J Neuro-Oncol 57(2):147–150
32. Chang CH, Huang WT, Kao CH, Chen SH, Lin CH (2013) Tetramethylpyrazine decreases hypothalamic glutamate, hydroxyl radicals and prostaglandin-E2 and has antipyretic effects. Inflamm Res 62(5):527–535. https://doi.org/10.1007/s00011-013-0606-3
33. Huang WT, Niu KC, Chang CK, Lin MT, Chang CP (2008) Curcumin inhibits the increase of glutamate, hydroxyl radicals and PGE2 in the hypothalamus and reduces fever during LPS-induced systemic inflammation in rabbits. Eur J Pharmacol 593(1–3):105–111. https://doi.org/10.1016/j.ejphar.2008.07.017
34. Chen SH, Oyarzabal EA, Hong JS (2013) Preparation of rodent primary cultures for neuron-glia, mixed glia, enriched microglia, and reconstituted cultures with microglia. Methods Mol Biol 1041:231–240. https://doi.org/10.1007/978-1-62703-520-0_21
35. Liu B, Hong JS (2003) Primary rat mesencephalic neuron-glia, neuron-enriched, microglia-enriched, and astroglia-enriched cultures. Methods Mol Med 79:387–395
36. Yu L, Quinn MT, Cross AR, Dinauer MC (1998) Gp91(phox) is the heme binding subunit of the superoxide-generating NADPH oxidase. Proc Natl Acad Sci U S A 95(14):7993–7998
37. Price MO, McPhail LC, Lambeth JD, Han CH, Knaus UG, Dinauer MC (2002) Creation of a genetic system for analysis of the phagocyte respiratory burst: high-level reconstitution of the NADPH oxidase in a nonhematopoietic system. Blood 99(8):2653–2661
38. Liu Y, Qin L, Wilson BC, An L, Hong JS, Liu B (2002) Inhibition by naloxone stereoisomers of beta-amyloid peptide (1-42)-induced superoxide production in microglia and degeneration of cortical and mesencephalic neurons. J Pharmacol Exp Ther 302(3):1212–1219. https://doi.org/10.1124/jpet.102.035956
39. Zhang X, Goncalves R, Mosser DM (2008) The isolation and characterization of murine macrophages. Curr Protoc Immunol Chapter 14:Unit 14 11. https://doi.org/10.1002/0471142735.im1401s83
40. Zhou H, Zhang F, Chen SH, Zhang D, Wilson B, Hong JS, Gao HM (2012) Rotenone activates phagocyte NADPH oxidase by binding to its membrane subunit gp91phox. Free Radic Biol Med 52(2):303–313. https://doi.org/10.1016/j.freeradbiomed.2011.10.488
41. Liu B, Du L, Hong J-S (2000) Naloxone protects rat dopaminergic neurons against inflammatory damage through inhibition of microglia activation and superoxide generation. J Pharmacol Exp Ther 293(2):607–617
42. Tan AS, Berridge MV (2000) Superoxide produced by activated neutrophils efficiently reduces the tetrazolium salt, WST-1 to

produce a soluble formazan: a simple colorimetric assay for measuring respiratory burst activation and for screening anti-inflammatory agents. J Immunol Methods 238(1–2):59–68
43. Romano J, Beni-Adani L, Nissenbaum OL, Brenneman DE, Shohami E, Gozes I (2002) A single administration of the peptide NAP induces long-term protective changes against the consequences of head injury: gene Atlas array analysis. J Mol Neurosci 18(1–2):37–45
44. Draye JP, Quintart J, Courtoy PJ, Baudhuin P (1987) Relations between plasma membrane and lysosomal membrane. 1. Fate of covalently labelled plasma membrane protein. Eur J Biochem 170(1–2):395–403
45. Zhang SC, Fedoroff S (1996) Neuron-microglia interactions in vitro. Acta Neuropathol 91(4):385–395
46. Gebicke-Haerter PJ, Bauer J, Schobert A, Northoff H (1989) Lipopolysaccharide-free conditions in primary astrocyte cultures allow growth and isolation of microglial cells. J Neurosci 9(1): 183–194
47. Talpain E, Armstrong RA, Coleman RA, Vardey CJ (1995) Characterization of the PGE receptor subtype mediating inhibition of superoxide production in human neutrophils. Br J Pharmacol 114(7):1459–1465
48. Kanamori Y, Niwa M, Kohno K, Al-Essa LY, Matsuno H, Kozawa O, Uematsu T (1997) Migration of neutrophils from blood to tissue: alteration of modulatory effects of prostanoid on superoxide generation in rabbits and humans. Life Sci 60(16):1407–1417
49. al-Essa LY, Niwa M, Kohno K, Nozaki M, Tsurumi K (1995) Heterogeneity of circulating and exudated polymorphonuclear leukocytes in superoxide-generating response to cyclic AMP and cyclic AMP-elevating agents. Investigation of the underlying mechanism. Biochem Pharmacol 49(3):315–322
50. Gao HM, Zhou H, Hong JS (2012) NADPH oxidases: novel therapeutic targets for neurodegenerative diseases. Trends Pharmacol Sci 33(6):295–303. https://doi.org/10.1016/j.tips.2012.03.008
51. Wang Q, Zhou H, Gao H, Chen SH, Chu CH, Wilson B, Hong JS (2012) Naloxone inhibits immune cell function by suppressing superoxide production through a direct interaction with gp91phox subunit of NADPH oxidase. J Neuroinflammation 9:32. https://doi.org/10.1186/1742-2094-9-32
52. Yu L, Zhen L, Dinauer MC (1997) Biosynthesis of the phagocyte NADPH oxidase cytochrome b558. Role of heme incorporation and heterodimer formation in maturation and stability of gp91phox and p22phox subunits. J Biol Chem 272(43):27288–27294
53. Qin L, Liu Y, Wang T, Wei SJ, Block ML, Wilson B, Liu B, Hong JS (2004) NADPH oxidase mediates lipopolysaccharide-induced neurotoxicity and proinflammatory gene expression in activated microglia. J Biol Chem 279(2):1415–1421. https://doi.org/10.1074/jbc.M307657200
54. Wilkinson BL, Landreth GE (2006) The microglial NADPH oxidase complex as a source of oxidative stress in Alzheimer's disease. J Neuroinflammation 3:30. https://doi.org/10.1186/1742-2094-3-30
55. Zhang W, Wang T, Qin L, Gao HM, Wilson B, Ali SF, Hong JS, Liu B (2004) Neuroprotective effect of dextromethorphan in the MPTP Parkinson's disease model: role of NADPH oxidase. FASEB J 18(3):589–591. https://doi.org/10.1096/fj.03-0983fje
56. Anantharam V, Kaul S, Song C, Kanthasamy A, Kanthasamy AG (2007) Pharmacological inhibition of neuronal NADPH oxidase protects against 1-methyl-4-phenylpyridinium (MPP+)-induced oxidative stress and apoptosis in mesencephalic dopaminergic neuronal cells. Neurotoxicology 28(5):988–997. https://doi.org/10.1016/j.neuro.2007.08.008